# Time-Invariant Stabilization of a Unicycle-Type Mobile Robot: Theory and Experiments

ByungMoon Kim[1] and Panagiotis Tsiotras[2]
*School of Aerospace Engineering*
*Georgia Institute of Technology, Atlanta, GA, 30332-0150*

## Abstract

In this paper we develop two time-invariant control laws for a unicycle-type mobile robot. A mobile robot of this type is an example of a system with a nonholonomic constraint. Similarly to the majority of results in the literature thus far, the controllers are based on the robot's kinematic model. They do not directly address realistic factors such as motor dynamics, quantization, sensor noise or delay which may affect the robot stability and performance. We use a Khepera robot to compare the performance of these controllers in a realistic situation that includes all the previous factors.

## Introduction

An underactuated system is one with fewer control inputs than independent generalized coordinates. Typically, underactuated systems arise because these generalized coordinates are subject to some non-integrable motion constraint, decreasing the degrees of freedom of the system, while the number of control inputs remains the same. These systems are called nonholonomic.

Several examples which involve nonholonomic constraints can be found in real world applications, such as mobile robots, bicycles, cars, underactuated axi-symmetric spacecraft, underwater vehicles, etc. Several control laws have been proposed for stabilizing such systems. One approach is to use time-varying controllers [6, 8, 5]. However, most of time-varying controllers have slow convergence rates [4]. Moreover, time-varying controllers may be non-robust to certain model perturbations [3]. Experimental validation of time-varying controllers has been performed in [6]. An alternative approach is to use time-invariant, non-smooth controllers, such as those in [9, 2, 1, 10]. These control laws ensure exponential convergence rates. Their robustness properties, however, is still a topic under investigation. This paper provides a small step towards this goal by providing some indication on the robustness properties of time-invariant, discontinuous controllers by implementing these controllers on a unicycle-type robot called Khepera. Ways to improve the controller performance are also discussed.

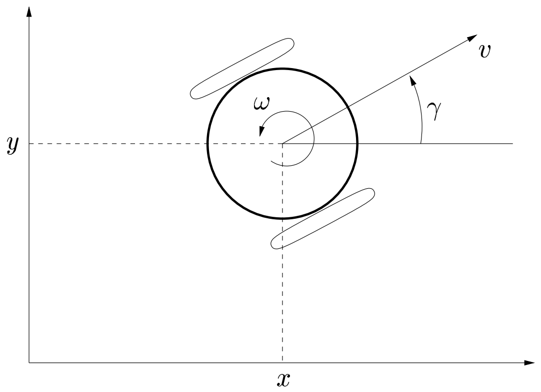

**Figure 1:** Definition of configuration variables.

## Kinematic Equations

Consider a unicycle-type robot with two wheels, as shown in Fig. 1. The kinematic equations are

$$\dot{x} = v\cos\gamma, \quad \dot{y} = v\sin\gamma, \quad \dot{\gamma} = \omega \tag{1}$$

The kinematic model of the mobile robot has two control inputs: velocity $v$ and angular velocity $\omega$ (see Fig. 1). Equation (1) can be transformed to a normal chained (or power) form by a state and input transformation. Using the state transformation

$$x_1 = x\cos\gamma + y\sin\gamma\,, \quad x_2 = \gamma \tag{2}$$

$$x_3 = x\sin\gamma - y\cos\gamma \tag{3}$$

one arrives at two slightly different systems, depending on the input transformation used. Systems I and II are given by

$$\text{(I)} \quad \begin{cases} \dot{x}_1 = u_1\,, \quad \dot{x}_2 = u_2\,, \quad \dot{x}_3 = x_1 u_2 \\ v = u_1 + x_3 u_2\,, \quad \omega = u_2 \end{cases} \tag{4}$$

$$\text{(II)} \quad \begin{cases} \dot{x}_1 = u_1 - x_3 u_2\,, \quad \dot{x}_2 = u_2\,, \quad \dot{x}_3 = x_1 u_2 \\ v = u_1\,, \quad \omega = u_2 \end{cases} \tag{5}$$

The two systems are completely equivalent when then inputs are $v$ and $\omega$ but are different when the inputs are $u_1$ and $u_2$. In particular, the two systems differ by the term $x_3 u_2$ in the $\dot{x}_1$ equation. Our experimental results show that this term has a significant effect in the transient response of the robot. This can be seen by observing that for System I angular velocity always generates forward velocity. In other words, for any control law $u_1$

[1] Graduate Student, E-mail: `gte342k@prism.gatech.edu`, Tel: (404) 894-9108, Fax: (404) 894-2760

[2] Associate Professor, E-mail: `p.tsiotras@ae.gatech.edu`, Tel: (404) 894-9526, Fax: (404) 894-2760. Corresponding author.

and $u_2$ that stabilizes System I, forward and angular velocities are coupled, a rather awkward condition. Also, for System I, large velocity commands may be generated when $x_3$ is large. Although it is easier to design a control law $u_1$ and $u_2$ using System I, its practical implementation favors System II. This fact has also been observed by McCloskey and Murray [6, 7] where they implemented their controllers (derived based on System I) using System II. Luckily, it turns out that the extra term $x_3 u_2$ does not destroy stability. A formal proof of the statement can be found in Proposition 2 below. Our experiments actually showed that working with System II was always beneficial.

### Controller 1

The first controller is given below

$$u_1 = -kx_1 + \beta_1(x,s), \qquad u_2 = -kx_2 + \beta_2(x,s) \quad (6)$$

where $\beta_1 = +\mu \dfrac{s(x)}{x_1^2 + x_2^2} x_2$ and $\beta_2 = -\mu \dfrac{s(x)}{x_1^2 + x_2^2} x_1$.

**Proposition 1** *The control law given by Eq. (6) globally asymptotically stabilizes System I for all initial conditions such that $x_1(0) \neq 0$ and $x_2(0) \neq 0$, if $\mu > 0$ and $k > 0$. Moreover, if $\mu > 2k > 0$ the control inputs $u_1$ and $u_2$ are bounded along the trajectories of the closed-loop system.*

**Proof:** The reader may refer to [2, 9] for the complete proof. ■

The derivation of the previous control law makes used of ideas from invariant manifold theory. Specifically, it can be shown that $\mathcal{M} = \{x \in \mathcal{R}^3 : s(x) = 0\}$ where $s(x) = x_3 - x_1 x_2/2$ is an invariant manifold for the closed-loop system. The nonlinear terms in (6) render $\mathcal{M}$ attractive and the linear terms drive any trajectory on $\mathcal{M}$ to the origin [9].

#### Singularity avoidance

The controller given by Eq. (6), is not defined on the $x_3$ axis. For initial conditions near the $x_3$ axis, large control inputs may result. A modification of controller (6) is needed for this singular case. To this end, let $|\eta| \equiv \sqrt{\beta_1^2 + \beta_2^2}/\mu = |s|/\sqrt{x_1^2 + x_2^2}$. Since the control input increases with $|\eta|$, this is a direct measure of the magnitude of the control input. Let us now denote the following neighborhood of the $x_3$ axis $\mathcal{D}_b = \{(x_1, x_2, x_3) : |\eta| \geq \eta_b\ \}$. The value $\eta_b$ is chosen by experimentation in order to achieve a reasonable control input and transient response. The set where $|\eta| < \eta_b$ will be denoted by $\mathcal{D}_b^c$. For initial conditions in the region $\mathcal{D}_b$ (where $|\eta|$ is large), we apply the following simple control law

$$u_1 = k_s \mathrm{sgn}(s), \quad u_2 = 0 \qquad (7)$$

to escape from $\mathcal{D}_b$, where $k_s$ is some constant. A simple argument shows that with the control law (7) the trajectories leave $\mathcal{D}_b$ in finite time. To complete the design of Controller 1, one must make sure that the control law given in Eq. (6) will not bring the closed-loop trajectory to the region $\mathcal{D}_b$. A simple calculation shows that $\dot{\eta} = -(\mu - 2k)/2\eta$ and $|\eta|$ is decreasing always under this control law. Thus, once the system leaves $\mathcal{D}_b$, it will never enter this region again.

We now turn our attention to System II. In this case, $s$ is not invariant under the simple feedback and one cannot apply the previous analysis to prove global asymptotic stability. However, local asymptotic stability can be shown using the properties of homogeneous systems. Before doing that, we show that the control law (6) achieves boundedness for the system in (5).

Consider the radially unbounded, positive definite function $V = x_1^2 + x_2^2 + x_3^2$. Its derivative along (5) and (6) is calculated as $\dot{V} = -2k(x_1^2 + x_2^2) \quad \leq 0$. This shows that $x_1 \to 0$, $x_2 \to 0$ as $t \to \infty$ and $x_3$ is bounded. To show local stability we need the following mathematical preliminaries.

**Definition 1** *For any set of positive scalars $r_i > 0$, $i = 0, \ldots, n$, the dilation operator $\Delta_\lambda^r$ is defined as $\Delta_\lambda^r x = [\lambda^{r_1} x_1\ \lambda^{r_2} x_2\ \ldots\ \lambda^{r_n} x_n]^T$ , $\lambda > 0$. The homogeneous norm associated with the dilation $\Delta_\lambda^r$ is a continuous function $\rho : \mathcal{R}^n \to \mathcal{R}_+$ if (i) $\rho(x) \geq 0$, and $\rho(x) = 0$ if and only if $x = 0$, and (ii) $\rho(\Delta_\lambda^r x) = \lambda \rho(x)$. Such a norm always exists.*

The next proposition basically states that the extra term $-x_3 u_2$ in the $\dot{x}_1$ equation for System II does not destroy asymptotic stability.

**Proposition 2** *The control law given by Eq. (6) locally asymptotically stabilizes the System II, if $k > 0$ and $\mu > 0$. Moreover, if $\mu > 2k$ the control law is bounded along the closed-loop trajectories.*

**Proof:** Let $f(x) = [u_1\ \ u_2\ \ x_1 u_2]^T$ and $g(x) = [-x_3 u_2\ \ 0\ \ 0]^T$, then the equation for System I is given by $\dot{x} = f(x)$ and the equation for System II is given by $\dot{x} = f(x) + g(x)$. The fact that the control law in (6) globally exponentially stabilizes the System I can be shown using the Lyapunov function $V(x_1, x_2, x_3) = \frac{1}{2}(x_1^2 + x_2)^2 + s^2$. The derivative of $V$ along the closed-loop trajectories of System I is given by $\dot{V} = L_f V(x) = -2k(x_1^2 + x_2^2)^2 - \mu s^2 \leq -\gamma V(x) < 0$ for all $x \in \mathcal{R}^3$, where $\gamma = \min\{4k, \mu\} > 0$. The derivative of $V$ along the closed-loop trajectories of System II is given by $\dot{V} = L_f V(x) + L_g V(x)$, where $L_g V(x) = -2(x_1^2 + x_2^2) x_1 x_3 u_2(x) + s x_2 x_3 u_2(x)$.

Consider the dilation $\Delta_\lambda^r x = [\lambda x_1\ \ \lambda x_2\ \ \lambda^2 x_3]^T$. Using this dilation, one obtains that $s(\Delta_\lambda^r x) = \lambda^2 s(x)$, $\beta_1(\Delta_\lambda^r x) = \lambda \beta_1(x)$ and $\beta_2(\Delta_\lambda^r x) = \lambda \beta_2(x)$. Therefore, $u_1(\Delta_\lambda^r x) = -k(\lambda x_1) + \lambda \beta_1(x) = \lambda u_1(x)$ and $u_2(\Delta_\lambda^r x) = -k(\lambda x_2) + \lambda \beta_2(x) = \lambda u_2(x)$. Thus, the control law in Eq. (6) is homogeneous of degree one with respect to the dilation $\Delta_\lambda^r x$. Moreover, since $L_f V(\Delta_\lambda^r x) = \lambda^4 L_f V(x)$ and $L_g V(\Delta_\lambda^r x) = \lambda^6 L_g V(x)$, then $L_f V$ and $L_g V$ are homogeneous functions of degrees four and six, respectively.

Consider now the homogeneous norm $\rho(x)$ associated with the given dilation $\Delta_\lambda^r$.[1] We claim that there exists

[1] Choose, for instance, $\rho(x) = (x_1^4 + x_2^4 + x_3^2)^{\frac{1}{2}}$.

$c > 0$ such that for all $\rho(x) \leq c$, $|L_f V(x)| > |L_g V(x)|$. To this end, let

$$\lambda^* = \min_{\rho(x)\leq 1} \sqrt{\frac{|L_f V(x)|}{|L_g V(x)|}} \qquad (8)$$

If $\lambda^* > 1$, let $c = 1$ and we are done. Otherwise, let a positive scalar $c^*$ such that $c^* < \lambda^* \leq 1$ and consider the set $\rho(x) \leq c^*$. Noticing that $\{\, x : \rho(x) \leq c^* \,\} = \{\, \Delta^r_\lambda y : \rho(y) \leq 1, \;\; 0 \leq \lambda \leq c^* \,\}$, one obtains that for any $x$ such that $\rho(x) \leq c^*$

$$\sqrt{\frac{|L_f V(x)|}{|L_g V(x)|}} = \sqrt{\frac{|L_f V(\Delta^r_\lambda y)|}{|L_g V(\Delta^r_\lambda y)|}} = \frac{1}{\lambda}\sqrt{\frac{|L_f V(y)|}{|L_g V(y)|}}$$

where $0 \leq \lambda \leq c^*$ and $\rho(y) \leq 1$. From (8) we have that

$$\frac{1}{\lambda}\sqrt{\frac{|L_f V(y)|}{|L_g V(y)|}} \geq \frac{\lambda^*}{\lambda} > 1$$

Since $x$ was arbitrary, this proves the assertion.
Therefore, there always exist a neighborhood of the origin such that $|L_f V(x)| > |L_g V(x)|$. Since $L_f V(x) < 0$, this implies that $\dot{V} = L_f V(x) + L_g V(x) < 0$ and System II is (at least) locally asymptotically stable.
To show that the control law remains bounded for $\mu > 2k > 0$ it suffices to show that $\eta$ remains bounded in a neighborhood of the origin. Along the trajectories of (5) with control law (6) we have that $\dot{s} = -(\mu/2)\, s + x_2 x_3 u_2/2$ and thus $\dot{\eta} = -[(\mu - 2k)/2]\, \eta + u_2 x_3 (4\nu^2 + \eta x_1)/(4\nu^2) = -[(\mu - 2k)/2]\, \eta + \phi(x)$. Next, notice that $\eta$ is homogeneous of degree one, whereas, $\phi(x)$ is homogeneous of degree three. Using a similar argument as before, we conclude that for a small enough neighborhood of the origin $\dot{\eta} < 0$ and the control law remains bounded around the origin. ■

## Controller 2

The second controller is based on a control law that was originally developed for the stabilization problem of an underactuated axisymmetric spacecraft [10]. It is modified here for the case of a mobile robot. In this controller, the control input is bounded by some finite value regardless of the initial conditions.
Consider the following controller,

$$u_i = -k \frac{x_i}{\sqrt{\nu^2 + 1}} + \mu \, \mathrm{sat_i}(s, \nu), \quad i = 1, 2 \qquad (9)$$

Where $\nu = \sqrt{x_1^2 + x_2^2}$ and the saturation functions $\mathrm{sat}_1$ and $\mathrm{sat}_2$ are defined as

$$\mathrm{sat}_{1,2}(s, \nu) = \begin{cases} \mathrm{sat}\left(\dfrac{s}{\nu}\right) \dfrac{x_{2,1}}{\nu}, & \text{if } \nu \geq \epsilon \\ \mathrm{sgn}(s), & \text{if } \nu < \epsilon \end{cases} \qquad (10)$$

with $\epsilon$ a small number to avoid chattering in the numerical implementation of the controller on a digital computer.

**Proposition 3** *The control law given by Eqs. (9) and (10) globally asymptotically stabilizes the System I for $k$ and $\mu$ satisfying $\mu > 2k > 0$ for $|\eta| < 1$ and $\mu > -2k > 0$ for $|\eta| \geq 1$[2]. Moreover, the control input is bounded by $|u_{1,2}| \leq |k| + \mu$.*

**Proof:** The proof involves two regions depending on the value of $\eta = s/\nu$. We investigate the closed-loop trajectories in the two regions of the state space $|\eta| < 1$ and $|\eta| \geq 1$. If $|\eta| < 1$, then $\mathrm{sat}_{1,2}(s, \nu) = (s/\nu^2)\, x_{2,1}$ and the time derivative of $s$ is $\dot{s} = -(\mu/2) s$. The time derivative of the radially unbounded, positive definite function $V_s \equiv x_1^2 + x_2^2 + s^2 = \nu^2 + s^2$ is therefore given by $\dot{V}_s = -2k\nu^2/\sqrt{\nu^2 + 1} - \mu s^2 < 0$. The time derivative of $\eta = s/\nu$, is computed as $\dot{\eta} = -(1/2)(\mu - 2k/\sqrt{\nu^2 + 1})\, \eta$. It follows that if $\mu > 2k$ the region where $|\eta| < 1$ is invariant. It follows that for all initial conditions in this region the state will remain in this region and converge to zero. This result shows that the closed-loop system will go to origin if the initial conditions satisfy $|\eta| < 1$. For $|\eta| \geq 1$, it is $\mathrm{sat}_{1,2}(s, \nu) = \mathrm{sgn}(s)(x_{2,1}/\nu)$ and the time derivative of $s$ is computed as $\dot{s} = -(1/2)\mu\nu \; \mathrm{sgn}(s)$. The time derivative of $\eta = s/\nu$ is thus computed as $\dot{\eta} = -(\mu/2) \; \mathrm{sgn}(s) + k\eta/\sqrt{\nu^2 + 1}$. Since $k < 0$, when $|\eta| \geq 1$, and since $\mathrm{sgn}(s) = \mathrm{sgn}(\eta)$ it follows that $|\eta|$ will always decrease and the trajectory will enter the region where $|\eta| < 1$ in finite time.
Combining the previous results, we see that the controller in Eq. (9) makes the closed loop trajectories converge to the origin for all initial conditions.
The fact that the control inputs are bounded by $|k| + \mu$ follows directly from (9). ■

Next, we apply Controller 2 to System II. For System II consider the radially unbounded, positive definite function $V = \frac{1}{2}(x_1^2 + x_2^2 + x_3^2)$. Its derivative is calculated as $\dot{V} = -k(x_1^2 + x_2^2)/\sqrt{x_1^2 + x_2^2 + 1}$. This result holds regardless whether $|\eta| < 1$ or $|\eta| \geq 1$. If $k > 0$, $V$ is non-increasing for all $x \in \mathcal{R}^3$. Thus, we conclude that $x_1$ and $x_2$ go to zero and $x_3$ is bounded. Moreover, since $-k(x_1^2 + x_2^2)/\sqrt{x_1^2 + x_2^2 + 1} \geq -k(x_1^2 + x_2^2 + x_3^2)/\sqrt{x_1^2 + x_2^2 + 1} \geq -kV$, it follows that $V$ is bounded below by an exponentially decaying function. Therefore, $x_1^2 + x_2^2$ go to zero asymptotically (not in finite time). Now, we have the following proposition.

**Proposition 4** *For $k > 0$ and $\mu > 0$, the control law in Eq. (9) and (10) globally asymptotically stabilizes the System II. Moreover, the control inputs are bounded by $|u_{1,2}| \leq k + \mu$.*

**Proof:** The proof is similar to the one of Proposition 3 and thus, omitted. It is based on the observation that $\dot{V} \leq 0$ only if $x_3$ converges to zero. ■

## Controller Implementation

The implementation of the controllers discussed previously was done on a Khepera mobile robot.

[2] The bound 1 is taken only for convenience. It could be any positive number.

Khepera is a small-size robot developed for educational and research purposes by K-Team (`http://www.k-team.com`). It has several proximity sensors (not used in this work) and can work in semi-autonomous (server-client) or completely autonomous mode. In the server-client mode the robot is controlled through an RS-232 serial port by a host computer. A C++ application running under Windows NT was developed to implement the previous algorithms and control the robot.

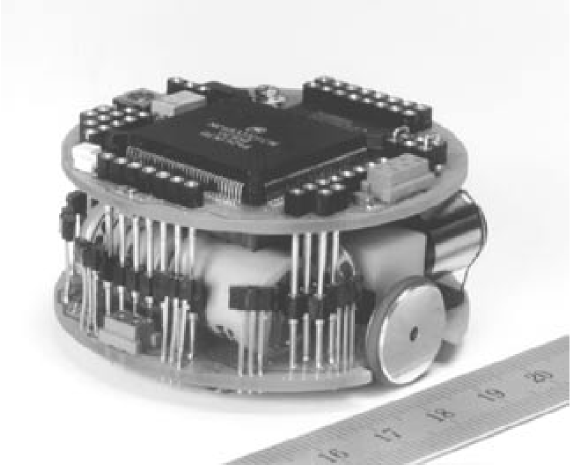

**Figure 2:** The Khepera robot (`http://www.k-team.com`).

### The Khepera Robot

The Khepera mobile robot uses two DC motor-driven wheels. The DC motors are connected to the wheels through a 25:1 reduction gear box. Two incremental encoders are placed on the motor axes. The resolution of the encoder is 24 pulses per revolution of motor axis. This corresponds to 24 × 25 = 600 pulses per revolution of the wheels or 12 pulses per millimeter of wheel displacement. The algorithm to estimate the velocity from the encoder output is implemented on the robot. For the DC motor speed control, a native PID controller is also implemented on the Khepera robot. All one needs to do in order to control Khepera, is to read position signals and issue velocity commands via the RS-232 serial port.

### Implementation of Controllers on a Windows NT Environment

C/C++ is used to implement the previous control algorithms with a nice-looking, multi-tabbed dialog box interface, shown in Fig. 3. From the `Realtime` tab, one can click the target position and orientation. The software automatically sets up a stabilizing problem by transforming the target position/orientation to origin and current position/orientation to the initial conditions. For the discrete implementation of the continuous controller, a 32bit multimedia timer service in NT is used and all other applications are closed to minimize the timer latency. The software provides a combo-box interface to select the sampling frequency of the controller in the `Configuration` tab. The maximum sampling rate can, theoretically, be slightly over 100Hz because of the speed limitation of the RS-232 serial communication (maximum is 4.8kbytes/s for the Khepera robot). For all experiments in this paper, we have chosen 50Hz for the sampling frequency. The software also features a `Sensors` display tab, and a `Console` tab. The motor can be tested/configured via the `Performance` tab. For convenience, all gains of the controller and other parameters are stored in a `.ini` file. The software comes also with an `ini` editor so that the user can change the settings online. To record the history of the control input and robot response without recording time limitations, a double-buffered data storage algorithm was developed. The robot can also be visualized by an independent OpenGL Window that supports 6DOF camera navigation using the keyboard.

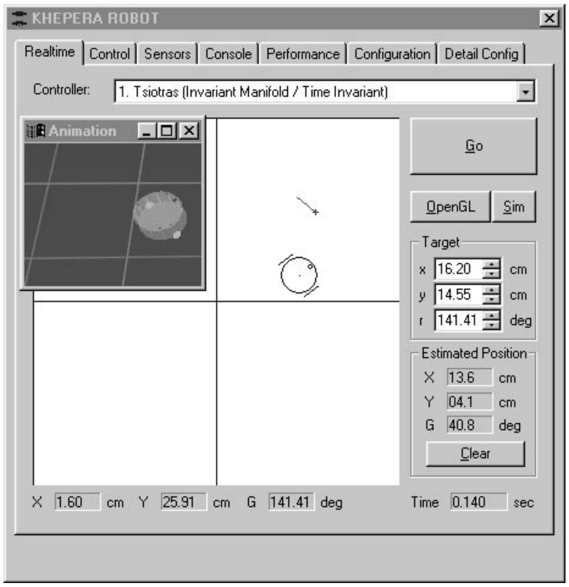

Controller: 1. Tsiotras (Invariant Manifold / Time Invariant)

Target
x 16.20 cm
y 14.55 cm
r 141.41 deg

Estimated Position
X 13.6 cm
Y 04.1 cm
G 40.8 deg

X 1.60 cm Y 25.91 cm G 141.41 deg Time 0.140 sec

**Figure 3:** Robot control program interface.

### Quantization in the Velocity Output

The velocity command of the Khepera robot is quantized by 8 mm/sec. At the origin, quantization is manifested as a deadzone problem. If we apply a control law, the small velocity command will be ignored by the robot and we will get large steady state errors. For example, the steady state error in $\gamma$ was about $15 \sim 60$ deg for both controllers. One simple but effective approach is to use an inverted deadzone to handle this problem. The responses of the robot with and without the inverted deadzone are shown in Fig. 4. A dramatic improvement in steady-state response (especially for $\gamma$) is achieved using this method. The inverted dead-zone is implemented in software.

### Scaling

Before implementing the controllers to the real robot, we need to choose the units of several variables, or more generally, to scale the states. By choosing the scaling values, we can adjust the magnitude of the states, i.e., $x_1, x_2$ and $x_3$. For each controller, state scaling was chosen to give the best transient response.

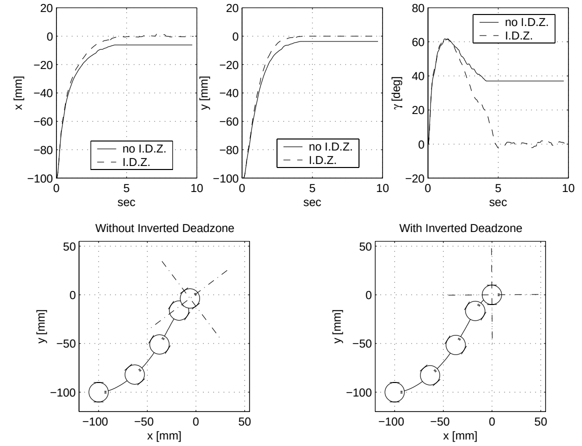

**Figure 4:** Effect of inverted deadzone on the steady state error

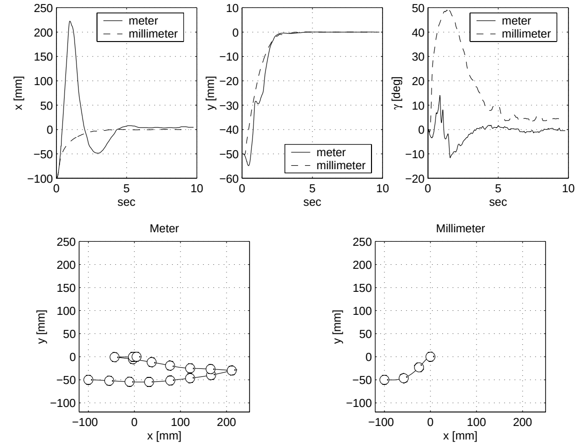

**Figure 5:** Comparison of responses with different units (scaling).

## Experimental Results

### Mission Design

To compare the two controllers, we designed four missions: easy, normal, singular and long distance. We defined the difficulty of each mission by the ratio between forward and sideways motions. The initial value of $\gamma$ is chosen to be zero. A long distance mission was devised to demonstrate the motor saturation due to possible large velocity commands. During the long distance mission the advantage of Controller 2 which has bounded input was evident. The initial conditions for these missions are shown in Table 1. Starting from this position, the robot is commanded to move to the origin.

**Table 1:** Mission specifications.

| Mission | x (mm) | y (mm) | $\gamma$ (deg) |
|---|---|---|---|
| Easy | -100 | -25 | 0 |
| Normal | -100 | -100 | 0 |
| Singular | 0 | -100 | 0 |
| Long Distance | -500 | -500 | 0 |

### Experimental Results

The summary of the experiments are shown in Table 2. In this table, 'E', 'N', 'S' and 'L' stand for easy, normal, singular and long distance missions, respectively. 'G' stands for 'Good', which means that the convergence is fast enough, i.e., within 10 seconds. 'O' stands for oscillatory, which means that the trajectory did not converge nor diverge but oscillated around the origin.

**Table 2:** Experimental results.

| Ctr. | Sys. | E | N | S | L | Note |
|---|---|---|---|---|---|---|
| 1 | I | G | O | O | O | Oscillatory |
| 1 | II | G | G | G | G | Good |
| 2 | I | G | G | G | O | Oscillatory |
| 2 | II | G | G | G | G | Good |

Figures 6 and 7 show plots of some selected trajectories. As it is shown in these figures, Controllers 1 and 2 may fail to achieve convergence for System I for some cases. In System II, they achieved stability for all missions.

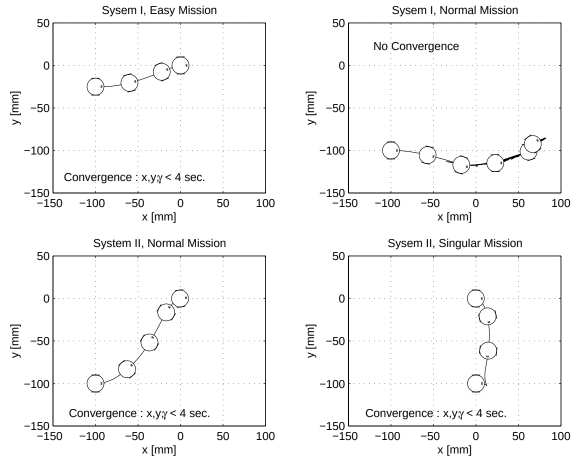

**Figure 6:** Selected Trajectories of Controller 1.

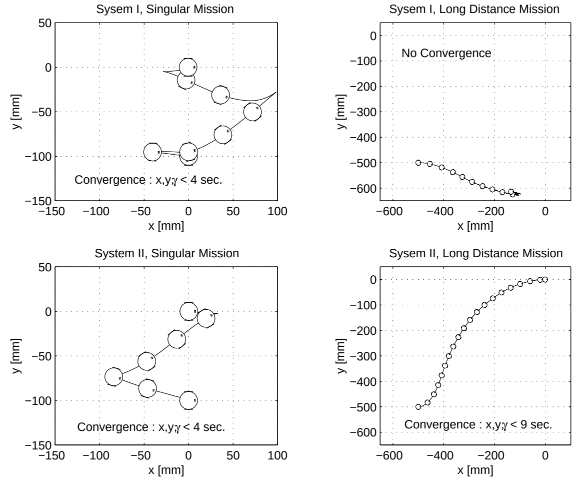

**Figure 7:** Selected Trajectories of Controller 2.

Figure 8 shows a comparison between the actual and commanded velocities for Controllers 1 and 2. The bounded Controller 2 behaves as expected, whereas, Controller 1 exhibits large magnitude in $v$. Figure 9 shows the commanded and actual forward and angular velocity responses for Systems I and II using the same controller (Controller 1) for the Normal mission. It is seen that a great improvement results in the commanded velocities using System II for controller implementation. In this case, Controller 1 exhibits highly oscillatory behaviour when applied to System I.

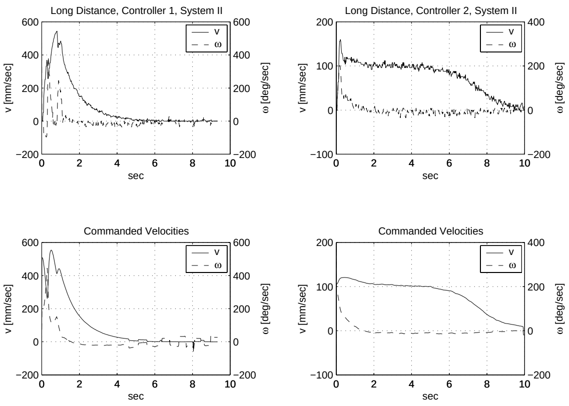

**Figure 8:** Selected Trajectories of Controller 2.

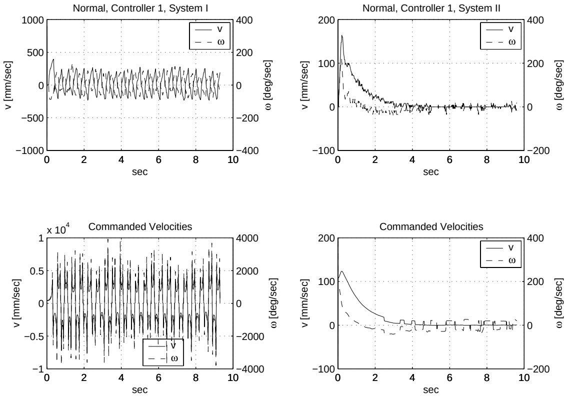

**Figure 9:** Commanded and Actual Velocities for Systems I and II.

More detailed plots of the results are available from the authors upon request.

## Conclusion

We have experimentally tested two time-invariant controllers for a unicycle-type mobile robot. These controllers are discontinuous at the origin so their experimental implementation/validation poses several interesting challenges. In particular, deadzone, quantization errors, sensor noise, poor measurements and motor dynamics can affect the response and even the stability of the system. We devised several techniques, such as input transformation, scaling and inverted deadzone to handle some of these issues. By applying these techniques, the performance improved significantly and the experimental results matched pretty closely to the theoretical predictions. Motor dynamics turned out to be a major problem for some tasks. Overall, the experiments showed that discontinuous, time-invariant controllers can be used successfully in practice if care is taken when implementing these controllers.

## References

[1] M. Aicardi, G. Casalino, A. Bicchi, and A. Balestrino, "Closed loop steering of unicycle-like vehicles via Lyapunov techniques," *IEEE Robotics and Automation Magazine*, Vol. 2, pp. 27–35, 1995.

[2] H. Khennouf and C. Canudas de Wit, "On the construction of stabilizing discontinuous controllers for nonholonomic systems," in *IFAC Nonlilear Control Systems Design Symposium*, pp. 747–752, 1995. Tahoe City, CA.

[3] D. A. Lizárraga, P. Morin, and C. Samson, "Non-robustness of continuous homogeneous stabilizers for affine control systems," in *38th IEEE Conference on Decision and Control*, pp. 855–860, 1999. Phoenix, AZ.

[4] R. T. M'Closkey and R. M. Murray, "Convergence rates for nonholonomic systems in power form," in *Proceedings of the American Control Conference*, pp. 467–473, 1993. San Francisco, California.

[5] R. T. M'Closkey and R. M. Murray, "Exponential convergence of nonholonomic systems: some analysis tools," in *Proceedings of the 31st Conference on Decision and Control*, pp. 943–948, 1993. San Antonio, Texas.

[6] R. T. M'Closkey and R. M. Murray, "Experiments in exponential stabilization of a mobile robot towing a trailer," in *Proceedings of the American Control Conference*, pp. 988–993, 1994. Baltimore, Maryland.

[7] R. T. M'Closkey and R. M. Murray, "Exponential stabilization of driftless nonlinear control systems using homogeneous feedback," *IEEE Transactions on Automatic Control*, Vol. 42, No. 5, pp. 614–628, 1997.

[8] A. R. Teel, R. M. Murray, and G. Walsh, "Nonholonomic control systems : From steering to stabilization with sinusoids," in *Proceedings of the 31st Conference on Decision and Control*, pp. 1603–1609, 1992. Tuckson, Arizona.

[9] P. Tsiotras and J. Luo, "Invariant manifold techniques for control of underactuated mechanical systems," in *Proceedings of the Workshop Modeling and Control of Mechanical Systems, Ed: A. Astolfi, P. J. N. Limebeer, C. Melchiorri, A. Tornambe, R. R. Vincer*, pp. 277–292, 1997. London, World Scientific Publishing Co.

[10] P. Tsiotras and J. Luo, "Stabilization and tracking of underactuated axisymmetric spacecraft with bounded control," in *IFAC Symposium on Nonlinear Control Systems Design (NOLCOS'98)*, 1998. Enschede, The Netherlands.